Journal of Physics:
Conference Series

PAPER • OPEN ACCESS

Multiphase boiling models of propane in a horizontal pipe: application of CFD techniques

To cite this article: Lorenzo Giunti *et al* 2025 *J. Phys.: Conf. Ser.* **2940** 012031

View the article online for updates and enhancements.

Multiphase boiling models of propane in a horizontal pipe: application of CFD techniques

Lorenzo Giunti[1], Federico Gigliotti[1], Francesco Giacomelli[2], Lorenzo Talluri[1] and Adriano Milazzo[1*]

[1] Department of Industrial Engineering, University of Florence, Italy
[2] Danfoss S.r.l., via Natale Salieri, 33-35, 40024 Castel San Pietro Terme, Bologna, Italy

*E-mail: adriano.milazzo@unifi.it

Abstract. This paper investigates the capabilities of CFD models, available in the commercial software Ansys, used in the study of the propane evaporation heat transfer coefficient trend. In particular, the flow in a horizontal pipe, at various average vapor qualities, has been considered. The scheme adopted in the definition of the problem is based on the Eulerian multiphase approach and RPI-CHF wall heat partitioning. A preliminary benchmark assessment, essential for validating the mathematical model, has been conducted with reference to boiling water in vertical pipes. The prediction is in consistent agreement with experimental results if a modification in some of the fundamental parameters is made. The validation has to be regarded as a propaedeutic study for future research related to more complex geometries, such as channels between corrugated plates of compact heat exchangers.

1. Introduction

The legislative requirements for environmental protection and concern about global climate change have prompted some countries to adopt measures towards a limitation in the use of Hydro-Fluoro-Carbon (HFC) refrigerants and alternative solutions which are more environmentally friendly.

Hydro-Carbons (HC) have been considered as real substitutes for HFCs as they show good thermodynamic and transport properties; in particular, propane (R290) has gained strong attention due to its physical characteristics similar to R22, with better heat transfer coefficient during the evaporation phase [1], ODP equal to 0 and GWP smaller than 3. Other advantages include compatibility with the majority of the HFCs-based equipment materials and miscibility with common compressor lubricants. Therefore, R290 represents a suitable choice for a charge switch.

The literature studies mainly give attention to the experimental test of performances of R290 in simple geometries. Wang et al. [2] carried out boiling heat transfer and frictional pressure gradient measurements in a smooth horizontal pipe at various saturation temperatures, heat and mass fluxes conditions. Choi et al. [3] and Maqbool et al. [4] reported the convective boiling pressure drops and local heat transfer coefficient HTC in horizontal and vertical mini-channels, respectively. Concerning more complex systems, the HTC during the vaporisation of R290 has been investigated by Longo [5] in a brazed plate heat exchanger with chevron corrugations, demonstrating substantial dependence on heat flux and outlet conditions.

Nevertheless, for a better physical understanding of the process and specific industrial applications, numerical simulations should be performed, developing new methods for multi-phase flows and computational techniques.

Chen et al. [6] provided an in-depth review of numerical simulations of boiling heat transfer, covering a wide range of scales, from the smallest to the largest relevant to the phenomenon, and emphasized the potential accuracy improvements achievable through a multi-scale approach. Specifically, Computational Fluid Dynamics (CFD) is a powerful tool capable of handling a broad spectrum of conditions, in terms of characteristic lengths and boiling heat transfer scenarios. Setoodeh et al. [7] developed a bubble dynamics model incorporating inertia- and thermal diffusion-controlled regimes to describe bubble growth within the Euler-Euler framework and validated it using experimental data from boiling flows of R12 refrigerant in a vertical pipe and R134a in an annular geometry. Colombo & Fairweather [8], adopting a similar approach, highlighted the need for improvements in modelling bubble break-up and coalescence phenomena, along with capturing the average velocities in the near-wall zone of annular channels, to obtain more reliable predictions. Končar & Krepper [9] conducted CFD simulations of R-113 flow in a vertical annular channel with an internally heated tube, showing that a two-phase wall function approach ensures a reasonable representation of the flow profiles at the wall. In the same context, few studies are devoted to propane boiling analysis. Qi et al. [10] employed a mathematical approach based on the k-ε turbulence model for the two-phase heat transfer of subcooled flow of R290 at low saturation temperature, in a 1.56 m long pipe. Dai et al. [11] used the Volume Of Fluid (VOF) methodology for exploring propane vapor-liquid flow behaviour in a horizontal smooth copper pipe.

In this paper, a novel numerical technique, implemented within the commercial software ANSYS Fluent 2022 R2, for predicting propane thermodynamics during the boiling process is presented.

The study of the phenomenon is divided into two cases, based on the initial temperature of the liquid: subcooled boiling, if it is below the saturation temperature and saturated boiling when the values are equal. In the latter case, the evolution of the flow regime inside the channel has also been taken into account, as it affects the heat transfer at the wall, approaching the single-phase convection with the onset of the dry-out condition. As depicted in Figure 1, the CFD model that is able to cover all the different situations is Critical Heat Flux, namely CHF-RPI, derived from the study of Kurul & Podowski [12] and implemented in the Eulerian multi-phase approach, which

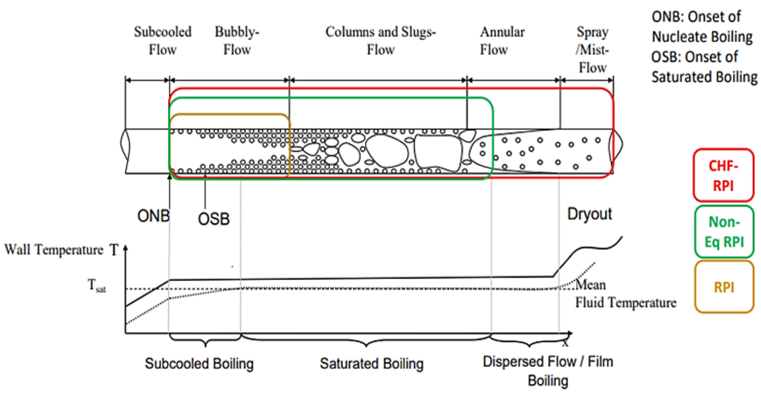

Figure 1. Boiling flow regimes and models applicability [13].

solves the governing equations for each phase, requiring correlations for the empirical closure of coefficients of the interfacial forces in the momentum balance.

2. Numerical methods and approaches

In this chapter, the mathematical and physical modelling used in this work is presented. The main specifications of the boiling model described hereafter are derived from the work done by Bianchini et al. [14] regarding the assessment of numerical procedures for multiphase heat transfer in different regimes.

2.1 Interfacial momentum equation terms

Four interfacial forces have been introduced during the analysis.

The Drag, as hydrodynamic friction between the liquid phase q and the dispersed phase p, is:

$$\vec{F}_D = K_{pq}\left|\vec{V}_p - \vec{V}_q\right| \tag{1}$$

where K_{pq} is proportional to a C_d coefficient, which was expressed by Ishi [15], selecting the lower value between the viscous regime and the distorted one.

The Lift, that pushes the small bubbles towards the wall, leading to void fraction peaking close but away from it, is:

$$\vec{F}_L = -C_L\alpha_p\rho_q(\vec{V}_q - \vec{V}_p) \times (\nabla \times \vec{V}_q) \tag{2}$$

where C_L is estimated with the Tomiyama correlation, modified by Frank et al. [16] and depends on the Eötvös number.

The Wall lubrication, instead, tends to prevent the bubbles from touching the solid surface, acting in the opposite direction to F_L and it is:

$$\vec{F}_W = C_{wl}\alpha_p\rho_q\left|\vec{V}_q - \vec{V}_p\right|^2_{\backslash\backslash}\vec{n}_w \tag{3}$$

with the subscript meaning that the velocity components are taken tangentially to the wall, whose unit normal is $\vec{n}_w$ and C_{wl} was determined by Antal [17].

Turbulent dispersion represents the impact of eddies in the continuous phase on the bubbles, and it promotes the homogenization of their distribution. The model proposed by Lopez de Bertodano [18] was applied:

$$\vec{F}_{td} = C_{td}\rho_q k_q \nabla\alpha_p \tag{4}$$

where k_q represents the turbulent kinetic energy in the continuous phase and C_{td} is a costant defaulting to a value of 1.

Finally, turbulence interaction between the induced one by particles and shear is formulated according to Troshko & Hassan [19] by adding the following source terms to the respective equations:

Journal of Physics: Conference Series **2940** (2025) 012031 doi:10.1088/1742-6596/2940/1/012031

$$\Pi_k = C_{ke} \sum K_{pq} \left|\vec{V}_p - \vec{V}_q\right|^2 \tag{5}$$

$$\Pi_\varepsilon = C_\varepsilon \frac{1}{\tau_p} \Pi_k \tag{6}$$

with $C_{ke} = 0.75$ and $C_\varepsilon = 0.45$, τ_p is the characteristic time of the induced turbulence.

2.2 Modelling of wall boiling

While the temperature of the vapor with the basic RPI model is not a result of the calculation but it is fixed at its saturation value, CHF-RPI treats it as an unknown variable, included in the solution process.

The entire heat flux transferred from the solid wall to the fluid is divided into four contributions:

$$\dot{q}_w = (\dot{q}_l + \dot{q}_q + \dot{q}_e) f(\alpha_l) + \dot{q}_v (1 - f(\alpha_l)) \tag{7}$$

The first term on the right-hand side is due to liquid-phase convection and it is:

$$\dot{q}_l = h_l (T_w - T_l)(1 - A_b) \tag{8}$$

followed by the quenching factor:

$$\dot{q}_q = \frac{2\lambda_l}{\sqrt{\pi \beta_l \tau}} (T_w - T_l) A_b \tag{9}$$

where λ_l is the conductivity, τ the bubble departure time and β_l is the liquid diffusivity.

Then, $\dot{q}_e$ is the component associated with evaporation:

$$\dot{q}_e = V_d N_w \rho_v h_{fv} f \tag{10}$$

V_d is the volume of the bubble which depends on the bubble departure diameter D_w, N_w is the active nucleate site density, h_{fv} is the latent heat of evaporation and $f = \tau^{-1}$.

The vapor phase convection $\dot{q}_v$ is analogous to $\dot{q}_l$. With A_b, the area fraction occupied by nucleating bubbles has been specified as, as:

$$A_b = \frac{K N_w \pi D_w^2}{4} \tag{11}$$

the constant K is calculated using Del Valle & Kenning's findings [20]. The release frequency f is based on an empirical correlation [21] as well as D_w [22].

The most relevant parameters in the analysis, as shown by the results in the next sections, are represented by N_w and the function $f(\alpha_l)$ which is based on the local liquid volume fraction α_l. The first one is usually expressed as follows:

$$N_w = C^n (T_w - T_{sat})^n \tag{12}$$

with $C = 210$ and $n = 1.805$ as proposed by Lemmert & Chawla [23].

Journal of Physics: Conference Series **2940** (2025) 012031
doi:10.1088/1742-6596/2940/1/012031

Tentner et al. [24] suggested the following definition for $f(\alpha_l)$:

$$1 - f(\alpha_l) = f(\alpha_v) = \begin{cases} 0 & \alpha_v < \alpha_{v1} \\ 0.5\left[1 - \cos\left(\pi \dfrac{\alpha_v - \alpha_{v1}}{\alpha_{v2} - \alpha_{v1}}\right)\right] & \alpha_{v1} \leq \alpha_v < \alpha_{v2} \\ 1 & \alpha_v \geq \alpha_{v2} \end{cases} \tag{13}$$

remembering that $\alpha_v = 1 - \alpha_l$.

Equation (13) shows that the heat flux terms in (7) are weighted by the relative local amount of vapor; the breakpoints are set to $\alpha_{v1} = 0.9$ and $\alpha_{v2} = 0.95$ by default, so $\dot{q}_w = \dot{q}_v$ for $\alpha_v \geq \alpha_{v2}$. In the standard RPI, $f(\alpha_l)$ is always equal to 1 and $\dot{q}_w = \dot{q}_l + \dot{q}_q + \dot{q}_e$.

3. Results and discussion

3.1 Validation of the model

To assess the adequacy of the simulation and acquire a deep understanding of how the model operates, RPI-CHF was preliminarily applied to two literature cases: the experiment of Bartolomej et al. [25] and Hoyer [26].

The former, which is illustrated in Figure 2a) together with boundary values, describes the sub-cooled boiling of water in a pipe whose internal diameter D_i is 15.4 mm and length $L = 2$ m; in the latter, measurements on externally heated pipes were carried out varying the diameter, mass flux and thermal power, the geometry selected is the one with $D_i = 10$ mm and $L = 7$ m and the data are shown in Figure 2b). In the second test section, a higher vapor volume fraction (VF) is achieved at the outlet implying the reaching of the critical flux region.

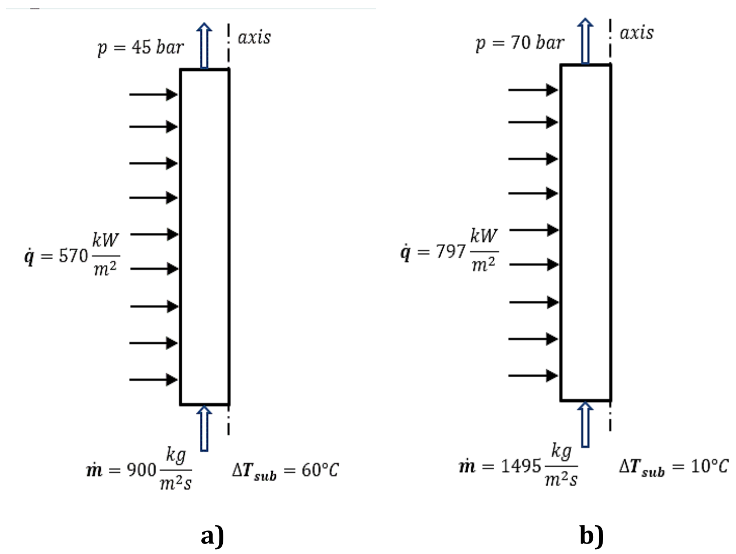

Figure 2. Experimental test sections schemes.

For both of them, a 2D axisymmetric computational domain has been created, meshed with hexahedral cells; a steady-state analysis has been conducted and liquid thermophysical properties have been varied with temperature, keeping saturation conditions constant along the pipe as the pressure level does not vary significantly. The mixture k-ω SST turbulence model was implemented. Negligible effects on the results were observed using either first or second-order discretization for each governing equation.

The profiles of the calculated VF at the centreline and wall temperature T_w, in simulating Bartolomej's case, are reported in Figure 3 for different models. Standard RPI reproduces quite well the real trend, even though it tends to slightly overestimate VF, while RPI-CHF fails in the prediction of T_w, even though it should be expected to have the same behaviour. A change could be brought by acting on N_w parameters, according to equation (12), and on an additional correction within the code that enhances the bubbles nucleation, getting better results with a redefined RPI-CHF modified.

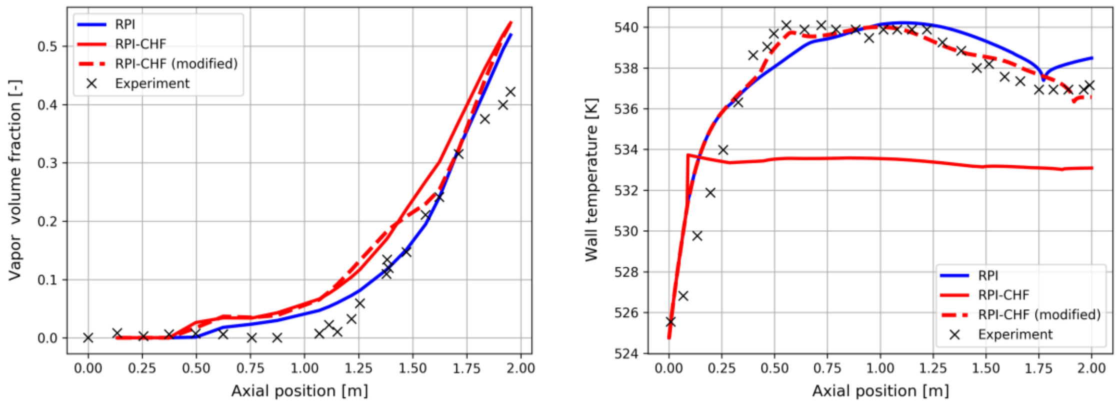

a) **b)**

Figure 3. Bartolomej et al. – Comparison of void fraction and wall temperature trends.

In Hoyer's test, the modified model seems to not match the experimental curve of wall temperature at higher VF, while RPI-CHF provides a consistent solution, properly identifying the position of dry-out, as depicted in Figure 4. However, in light of the foregoing and considering the whole range of vapor qualities which can be experienced in an evaporator, RPI-CHF is the most appropriate approach to adequately represent the boiling process.

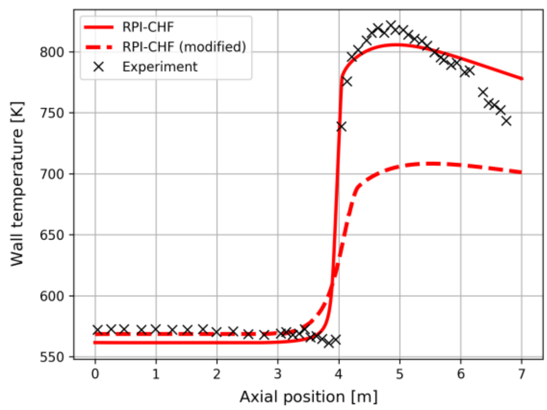

Figure 4. Hoyer – Comparison of wall temperature trends.

To provide a clearer understanding of the key differences between the models described above, their main characteristics are listed in Table 1. This summary highlights the distinct features of each model, enabling a comparison of their functionality.

Table 1. Characteristics of RPI-based models.

	Wall treatment	Description
Standard	$\dot{q}_w = \dot{q}_l + \dot{q}_q + \dot{q}_e$	Vapor temperature set to its saturation value
CHF	$\dot{q}_w = (\dot{q}_l + \dot{q}_q + \dot{q}_e)f(\alpha_l) + \dot{q}_v(1 - f(\alpha_l))$	Convective heat flux of the vapor phase included
CHF (modified)	$\dot{q}_w = (\dot{q}_l + \dot{q}_q + \dot{q}_e)f(\alpha_l) + \dot{q}_v(1 - f(\alpha_l))$	Bubble nucleation enhancement deactivated

3.2 Boiling propane analysis

The test rig studied by Allymehr [27] has been selected: he measured the heat transfer coefficient (HTC) of R290 at various average vapor qualities x, setting the inlet saturation temperature, mass flow rate and heat flux in a system with a smooth copper pipe electrically heated, located at Thermal lab of the Department of Energy and Process Engineering of Norwegian University of Science and Technology.

The computational domain consists of the solid geometry and fluid volume, meshed with polyhedral elements, adding a proper number of inflations layers near the wall to ensure getting dimensionless distance y^+ greater than 30 as a general recommendation for wall functions in boiling cases [13], with the mixture k-ω SST turbulence model implemented.

The pipe, with $D_i = 4.2$ mm and $L = 0.5$ m, has been lengthened upstream of the inlet section to allow flow stratification, as illustrated in Figure 5 for one of the eight simulated test points, and backward heat diffusion. Due to gravity, the liquid settles down at the bottom where the VF is lower than at the top, the difference between these two values becomes smaller approaching the outlet and increasing x too, with a minimum experienced by the last point having everywhere $VF > 0.99$.

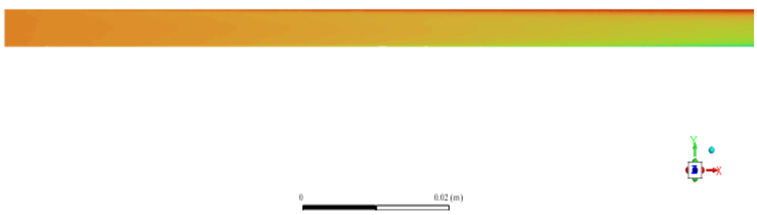

Figure 5. Vapor volume fraction contour in the adiabatic entrance.

Conjugate heat transfer calculations in steady state were executed with an imposed heat flux at the external surface and boundary conditions as listed in Table 2; vapor quality x_{in} at the inlet has been determined by the relationship between x_{in}, $\dot{q}_w$, h_{fv} and G knowing x, with $x = x_{in} + 0.5\Delta x$; pressure at the outlet has been derived from pressure drops.

Table 2. Boundary conditions for the investigated scenario.

	Variable	Unit of measure	Value
Inlet temperature	T_{sat}	°C	5
Mass flux	G	kg/(m²s)	379.41
Internal heat flux	$\dot{q}_w$	kW/m²	31.88

With the default settings for the blending function $f(\alpha_l)$, breakpoints and nucleate site density, the model is not able to correctly match the HTC trend for $0.1 < x < 0.7$, indeed dry-out occurs at a quality less than expected and T_w rises along the pipe, reaching a high value near the outlet section.

Therefore, a modification to the blending function has been made to delay the situation of single-phase convection with vapor only and N_w parameters have been adjusted to avoid wall temperature underestimation. This is also justified by the fact that almost all the implemented boiling definitions are valid for water in vertical channels. Figure 6 presents the CFD results for the HTC trend and error, compared with the experimental data.

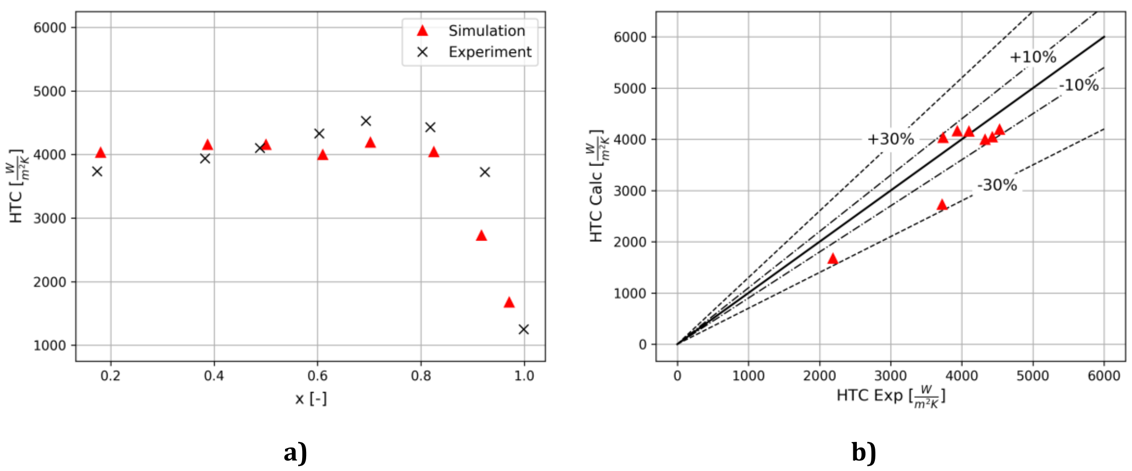

Figure 6. Comparison between calculated and experimental HTC.

As shown in Figure 6a), the location of HTC maximum and its following drop for $x > 0.7$, is well reproduced. The most significant component in Equation (7) is $\dot{q}_e$ being beyond 60% of $\dot{q}_w$ since $x < 0.8$; it grows for $0.1 < x < 0.7$ and starts to decrease for $x > 0.8$, with the process that becomes driven by single-phase convection with vapor. The lower wall temperature reached at HTC maximum is the reason for liquid heat transfer reduction in the above-mentioned range, even if the velocity is higher as the flow rate is fixed. The quenching factor is the second most significant contribution at the lowest x when $\dot{q}_v$ is nearly zero.

HTC errors are less than 10% regarding the first six test points and the greatest one is about 26% at $x = 0.92$.

4. Conclusions

In the present work, an investigation of current available CFD multiphase models for testing boiling propane in a horizontal pipe has been proposed, with the specific goal of assessing the most relevant characteristics affecting the solution.

A good qualitative agreement was found with the experiments even though a proper change of default settings has to be applied, taking into account the difference in both the arrangement and the type of fluid considered to calibrate the fundamental correlations and values on which the scheme is based.

An accurate analysis of the wall heat flux partitioning and the weight of individual terms has been performed, to comprehend the basics of the transfer phenomenon and identify how it operates.

Future research is necessary to extend the calculation to other wall heat and mass flux conditions and to evaluate more suitable sub-model equations, like bubble departure diameter and release frequency, for R290.

References

[1] Granryd E., 2001, *Hydrocarbons as refrigerants*, International Journal of Refrigeration, Vol. 4, pp. 15-24
[2] Wang S., Gong M. Q., Chen G. F., Sun Z. H., 2014, *Two-phase heat transfer and pressure drop of propane during saturated flow boiling inside a horizontal tube*, International Journal of Refrigeration, Vol. 41, pp. 200-209
[3] Choi K., Pamitran A. S., Oh J., Saito K., 2009, *Pressure drop and heat transfer during two-phase flow vaporization of propane in horizontal smooth minichannels*, International Journal of Refrigeration, Vol. 32, pp. 837-845
[4] Maqbool M. H., Palm B., Khodabandeh R., 2013, *Investigation of two phase heat transfer and pressure drop of propane in a vertical circular minichannel*, Experimental Thermal and Fluid Science, Vol. 46, pp. 120-130
[5] Longo G. A., 2010, *HC-290 (Propane) Vaporisation Inside a Brazed Plate Heat Exchanger*, International Refrigeration and Air Conditioning Conference, paper 1009
[6] Chen Y., Yu B., Lu W., Wang B., Sun D., Jiao K., Zhang W., Tao W., 2024, *Review on numerical simulation of boiling heat transfer from atomistic to mesoscopic and macroscopic scales*, International Journal of Heat and Mass Transfer, Vol. 225, paper 125396
[7] Setoodeh H., Ding W., Lucas D., Hampel U., 2021, *Modelling and simulation of flow boiling with an Eulerian-Eulerian approach and integrated models for bubble dynamics and temperature-dependent heat partitioning*, International Journal of Thermal Sciences, Vol. 161, paper 106709
[8] Colombo M., Fairweather M., 2016, *Accuracy of Eulerian–Eulerian, two-fluid CFD boiling models of subcooled boiling flows*, International Journal of Heat and Mass Transfer, Vol. 103, pp. 28-44
[9] Končar B., Krepper E., 2008, *CFD simulation of convective flow boiling of refrigerant in a vertical annulus*, Nuclear Engineering and Design, Vol. 238, pp. 693-706
[10] Qi D., Zhang J., Gao W., 2020, *Numerical Study on Two-Phase Heat Transfer and Flow of Subcooled Flow Boiling of R290 in A Vertical Tube*, World Scientific Research Journal, Vol. 6, Issue 7
[11] Dai Y., Zhang N., Tian S., Du H., 2020, *Numerical study of flow boiling heat transfer of propane in a horizontal smooth copper tube*, Heat Transfer Research, Vol. 51, pp. 1653-1667
[12] Kurul N., Podowski M. Z., 1991, *On the Modeling of Multidimensional Effects in Boiling Channels*, In Proceedings of the 27th National Heat Transfer Conference, Minneapolis, USA
[13] ANSYS Fluent Learning Hub, ANSYS, Inc., Canonsburg, PA

[14] Bianchini C., Da Soghe R., Mazzei L., Caggiano G., Angelucci M., 2021, *Assessment of CFD Models for Multiphase Heat Transfer in Different Boiling Regimes*, Proceedings of ASME Turbo Expo 2021, Turbomachinery Technical Conference and Exposition, GT2021

[15] Ishii M., 1979, *Two-fluid model for two-phase flow*, 2nd International Workshop on Two-phase Flow Fundamentals, RPI, Troy, NY

[16] Frank T., Shi J. M., Burns A. D., 2004, *Validation of Eulerian Multiphase Flow Models for Nuclear Safety Applications*, 3rd International Symposium on Two-Phase Flow Modeling and Experimentation, Pisa, Italy

[17] Antal S. P., Lahey R. T., Flaherty J. E., 1991, *Analysis of phase distribution in fully developed laminar bubbly two-phase flow*, International Journal of Multiphase Flow, Vol. 17, pp. 635–652

[18] Lopez de Bertodano M., 1991, *Turbulent Bubbly Flow in a Triangular Duct,* Ph.D. Thesis, RPI, Troy, New York

[19] Troshko A., Hassan Y. A., 2001, *A Two-Equation Turbulence Model of Turbulent Bubbly Flow*, International Journal of Multiphase Flow, Vol. 27, pp. 1965–2000

[20] Del Valle V. H., Kenning D. B. R., 1985, *Subcooled flow boiling at high heat flux*, International Journal of Heat and Mass Transfer, Vol. 28, pp. 1907–1920

[21] Cole R., 1960, *A Photographic Study of Pool Boiling in the Region of the Critical Heat Flux*, AIChE, Vol. 6, pp. 533-538

[22] Tolubinski V. I., Kostanchuk D. M., 1970, *Vapor bubbles growth rate and heat transfer intensity at subcooled water boiling*, 4th International Heat Transfer Conference, Paris, France

[23] Lemmert M., Chawla L. M., 1977, *Influence of flow velocity on surface boiling heat transfer coefficient in Heat Transfer in Boiling*, E. Hahne and U. Grigull (Eds.), Academic Press and Hemisphere, New York, USA

[24] Tentner A., Lo S., Kozlov V., 2006, *Advances in Computational Fluid Dynamics Modeling of Two Phase Flow in a Boiling Water Reactor Fuel Assembly*, International Conference on Nuclear Engineering, Miami, Florida

[25] Bartolomei G. G., Brantov V. G., Molochnikov Yu. S., Kharitonov Yu. V., Solodkii V. A., Batashova G. N., Mikjailov V. N., 1982, *An experimental investigation of true volumetric vapor content with subcooled boiling in tubes*, Thermal Engineering, Vol. 29, pp. 132–135

[26] N. Hoyer, 1998, *Calculation of dryout and post-dryout heat transfer for tube geometry*, International Journal of Multiphase Flow, Vol. 24, pp. 319-334

[27] Allymehr E., 2017, *Experimental Investigation of evaporation of propane (R290) in small pipes*, Master Thesis, School of Industrial and Information Engineering, Milano